

Ab Initio Calculations of the Electron-Transfer Matrix Element in Cu^I–Cu^{II} Mixed-Valence Compounds

Carmen Jiménez Calzado and Javier Fernández Sanz*

Contribution from the Departamento de Química Física, Facultad de Química, Universidad de Sevilla, E-41012, Sevilla, Spain

Received July 21, 1997. Revised Manuscript Received November 24, 1997

Abstract: A theoretical analysis of the electron-transfer matrix element, V_{ab} , for some cluster models intended to mimic the properties of the [NEt₄][Cu₂Cl₄] mixed-valence compound prepared by Willet et al.¹ is reported. On the basis of ab initio unrestricted Hartree–Fock calculations, both V_{ab} and the potential energy profiles versus an idealized electron-transfer reaction coordinate have been calculated for different scenarios. Our best estimate for V_{ab} is found to be 971 cm⁻¹ in agreement with experimental related work. The physical factors governing the amplitude of the electronic coupling as well as the shape of the energy profiles have been analyzed. It is shown that in order to account for a correct type II behavior within the Robin–Day classification, the polarization effects induced on the cluster by the environment have to be included. The dependence of V_{ab} on the nature of the ligands bridging the Cu^I–Cu^{II} centers is discussed. Our results for a family of compounds of formula [Cl₂Cu^IX₂Cu^{II}Cl₂]³⁻ (X = Cl⁻, OH⁻, SH⁻) show that both V_{ab} and the energy profiles are largely dependent on the nature of X.

1. Introduction

Properties of copper mixed-valence compounds presently constitute one of the most appealing subjects both in biochemistry and inorganic chemistry. For instance, the Cu^I–Cu^{II} pair is found in biological systems such as hemocyanin derivatives,² cytochrome *c* oxidase,³ or nitrous oxide reductase.⁴ The same pair is also found in cerium-doped Nd₂CuO₄ oxides which are the basis of a family of high-temperature superconductors.⁵ From a structural point of view, the most outstanding aspect of these bimetallic mixed-valence compounds is the presence of two metal centers which under specific conditions are able to interchange their formal oxidation state through an electron-transfer process.

In 1987 Willett reported¹ on the preparation of a Cu^I–Cu^{II} mixed-valence compound of formula [NEt₄][Cu₂Cl₄] in which the two nonequivalent copper centers are bridged by two chloride ions. This compound was shown to form linear chains with semiconductive behavior and characterized as belonging to the Robin and Day class II.⁶ In a later work,⁷ the synthesis and characterization of bromide derivatives were also reported. The low dimensionality of these compounds makes them especially suitable for theoretical analysis as noted by Sherwood and Hoffmann⁸ who performed a study of the band structure of

[NEt₄][Cu₂Cl₄] showing its Peierls-distorted nature with a strongly trapped charge density wave.

The conductive properties of these chains can be viewed from a local point of view as arising from a concerted electron jump between Cu^I and Cu^{II} centers, i.e., as a simultaneous and generalized electron-transfer reaction. As is well-known, most of the long-distance electron-transfer (ET) reactions are considered as nonadiabatic processes, for which, according to the Golden Rule,⁹ the rate constant expression is written as

$$k_{ET} = \left(\frac{\pi}{\hbar^2 \lambda_s k_B T} \right)^{1/2} |V_{ab}|^2 e^{-\Delta G^\ddagger/k_B T} \quad (1)$$

where λ_s is the reorganization energy of the ET step, V_{ab} is the electronic coupling matrix element between two diabatic states, **a** and **b**, and ΔG^\ddagger is the free activation energy. Within the framework of the two-states model, V_{ab} is conventionally defined as half the splitting between the adiabatic potential energy surfaces at the crossing seam, and plays a pivotal role in the theory of the ET reactions, since besides its participation in the expression for the rate constant, the magnitude of the electronic coupling determines whether an ET process is adiabatic or nonadiabatic.

Qualitatively, the properties of mixed-valence compounds are usually rationalized on the basis of the Robin and Day

(1) Willet, R. D. *Inorg. Chem.* **1987**, *26*, 3423.

(2) (a) Solomon, E. I. *Copper Proteins*. Spiro, T. G., Ed.; Wiley: New York, 1981. (b) Westmoreland, T. D.; Wilcox, D. E.; Baldwin, M. J.; Mims, W. B.; Solomon, E. I. *J. Am. Chem. Soc.* **1989**, *111*, 6106.

(3) Farrar, J. A.; Neese, F.; Lappalainen, P.; Kroneck, P. M. H.; Saraste, M.; Zumft, W. G.; Thomson, A. J. *J. Am. Chem. Soc.* **1996**, *118*, 11501.

(4) Neese, F.; Zumft, W. G.; Antholine, W. E.; Kroneck, P. M. H. *J. Am. Chem. Soc.* **1996**, *118*, 8692.

(5) Bednorz, J. G.; Müller, K. A. *Earlier and Recent Aspects of Superconductivity*; Springer, New York, 1990. Cox, P. A. *Transition Metal Oxides: An introduction to their electronic structure and properties*; Clarendon Press: Oxford, 1995.

(6) Robin, M. B.; Day, P. *Adv. Inorg. Chem. Radiochem.* **1967**, *10*, 247.

(7) Scott, B.; Willet, R. D.; Porter, L.; Williams, J. *Inorg. Chem.* **1992**, *31*, 2483.

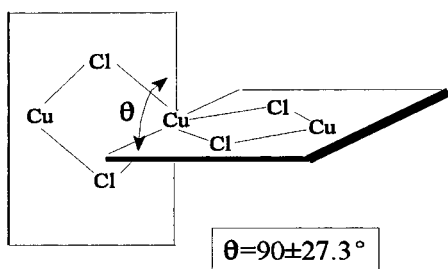
(8) Sherwood, P.; Hoffmann, R. *Inorg. Chem.* **1989**, *28*, 509.

(9) (a) Newton, M. D. *Chem. Rev.* **1991**, *91*, 767. (b) Mikkelsen, K. V.; Ratner, M. A. *Chem. Rev.* **1987**, *87*, 113. (c) Cannon, R. D. *Electron-Transfer Reactions*, Butterworth: Stoneham, MA, 1980. (d) Marcus, R. A. *J. Chem. Phys.* **1956**, *24*, 966; *Can. J. Chem.* **1959**, *37*, 155; *Discuss. Faraday Soc.* **1960**, *29*, 21; *J. Annu. Rev. Phys. Chem.* **1964**, *15*, 155; *J. Chem. Phys.* **1965**, *43*, 679; *Electrochim. Acta* **1968**, *13*, 995. (e) Brunshwig, B. S.; Logan, J.; Newton, M. D.; Sutin, N. *J. Am. Chem. Soc.* **1980**, *102*, 5798. (f) Levich, V. G. *Adv. Electrochem. Electrochem. Eng.* **1966**, *4*, 249. (g) Dogonadze, R. R.; Kuznetsov, A. M.; Levich, V. G. *Electrochim. Acta* **1968**, *13*, 1025. (h) Kestner, N. R.; Logan, J.; Jortner, J. *J. Phys. Chem.* **1974**, *78*, 2148. (i) Ulstrup, J.; Jortner, J. *J. Chem. Phys.* **1975**, *63*, 4358. (j) Efrima, S.; Bixon, M. *Chem. Phys.* **1976**, *13*, 447. (k) Can Duynne, R. P.; Fischer, S. F. *Chem. Phys.* **1974**, *13*, 183.

classification according to their potential surface shapes, whose features can be roughly estimated by taking into account the electronic coupling between the diabatic states and the reorganization energy. In a recent work, we reported¹⁰ on an estimate for the electronic coupling for the $[\text{Cu}_2\text{Cl}_6]^{3-}$ system as an application of a procedure to build up dedicated molecular orbitals specially tailored to compute the observable V_{ab} from configuration interaction (CI) calculations within a 2×2 effective Hamiltonian frame.¹¹ In the present paper we report on a theoretical study of the main factors governing the size of V_{ab} and the shape of the potential energy surfaces. For this purpose, energy profiles for both diabatic and adiabatic states along idealized electron-transfer reaction coordinates have been computed. The work is mainly addressed to the $[\text{NEt}_4][\text{Cu}_2\text{Cl}_4]$ Willett system, in which the two copper centers are bridged by two chloride ions, however, to analyze the influence of the ligands, some models in which the copper ions are bridged through OH^- and SH^- ligands will also be considered. Because the computation of the electronic coupling at the CI level as reported in refs 10 and 11 is too cumbersome for a systematic study, the calculations in this work have been performed by exploiting the unrestricted Hartree-Fock broken-symmetry wave functions as implemented in the HONDO 8.4 program.¹²

2. Models

The structure of $[\text{NEt}_4][\text{Cu}_2\text{Cl}_4]$ reported by Willet et al. can be described as a chain of CuCl_4 tetrahedra sharing edges, with a repeat unit of four copper atoms (Figure 1). In this chain there are two nonequivalent copper sites with different Cu-Cl lengths. Cu^{II} ions are on sites with D_2 local symmetry, and exhibit shorter Cu-Cl distances than those of Cu^{I} centers which are on sites with D_{2d} local symmetry. The D_2 local geometry is close to the flattened tetrahedral D_{2d} structure arising from Jahn-Teller distortion of CuCl_4^{2-} ion, but with a CuCl_2 plane rotated by 27.3° , while the D_{2d} centers result from a compression of the CuCl_2 angle at the Cu^{I} site from the tetrahedral value to 93° .



To model the $\text{Cu}^{\text{I}}-\text{Cu}^{\text{II}}$ system of this chain we have selected a cluster of formula $\text{Cu}_2\text{Cl}_6^{3-}$ which is the same unit used by Sherwood and Hoffmann in their extended Huckel MO band calculations. Basically it consists of two CuCl_2 subunits bridged by two chloride ligands with a Cu-Cu distance fixed to 3.1 \AA according to the experimental data. Two possibilities were considered. In the first one, the bridge plane is assumed to be perpendicular to the ending CuCl_2 units (model I-Cl) and, therefore, the metal centers have D_{2d} local symmetry. In the second model (model II-Cl), the bridge plane is taken to be the

(10) Calzado, C. J.; Sanz, J. F.; Castell, O.; Caballol, R. *J. Phys. Chem. A* **1997**, *101*, 1716.

(11) Sanz, J. F.; Malrieu, J. P. *J. Phys. Chem.* **1993**, *97*, 99.

(12) Dupuis, M.; Chin, S.; Márquez, A. CHEM-Station and HONDO: Modern Tools for Electronic Structure Studies Including Electron Correlation. In *Relativistic and Electron Correlation Effects in Molecules and Clusters*; Mali, G. L., Ed.; NATO ASI Series; Plenum Press: New York, 1994.

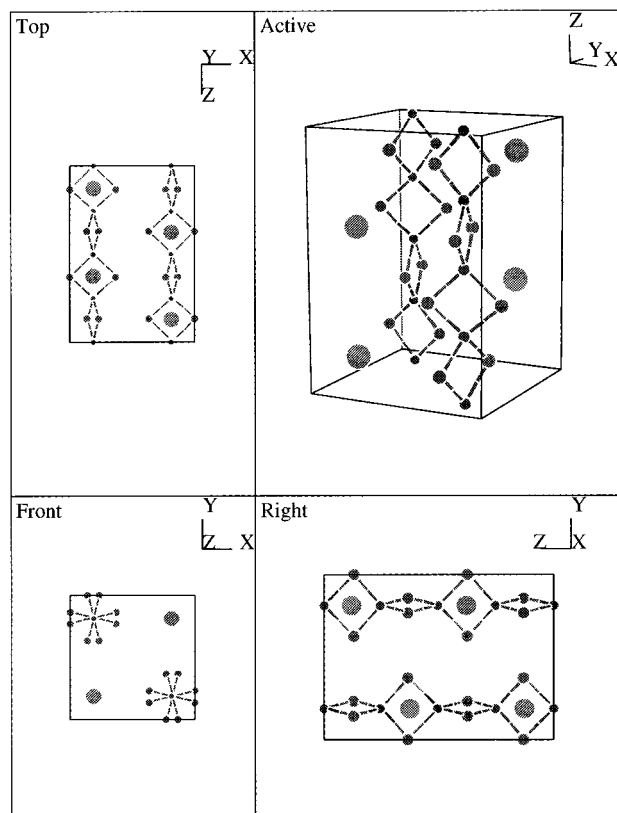


Figure 1. Unit cell for $[\text{NEt}_4][\text{Cu}_2\text{Cl}_4]$ compound. The tetraethylammonium cations are represented by isolated spheres.

same as that of the ending CuCl_2 units and thus, the local symmetry on the metal centers is almost D_{4h} . Notice that unless at the crossing seam configuration, the metals are not equivalent and that the full symmetry is C_{2v} . The bond distances and bond angles of these clusters have been idealized according to the experimental data and have been summarized in Table 1. Also, with the aim of examining the features of models closer to that of the Willett system, we have also performed a series of calculations in which the dihedral angle θ between the $\text{Cu}^{\text{I}}-\text{Cl}_2$ planes has been varied. These twisted models will be labeled as t-Cl (Figure 2).

On the other hand, to investigate the effects due to the ligand nature on the electron-transfer matrix element in the $\text{Cu}^{\text{I}}-\text{Cu}^{\text{II}}$ system, two more different bridges were considered. In these models, the chlorides bridging the CuCl_2 units are replaced by OH^- and SH^- groups. This replacement gives rise to four models more that will be denoted as I-OH, I-SH, II-OH, and II-SH (see Figure 2). The geometry of these models were idealized using the covalent radii of the bridge atoms, keeping the $\text{Cu}^{\text{I}}-\text{Cu}^{\text{II}}$ distance always fixed at 3.1 \AA (Table 1).

3. Computational Methods

The general procedure to compute the electron-transfer matrix element, V_{ab} , in the present work is the so-called direct procedure according to which, and within the two-states model,¹³ V_{ab} is computed at the crossing seam as

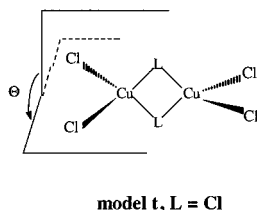
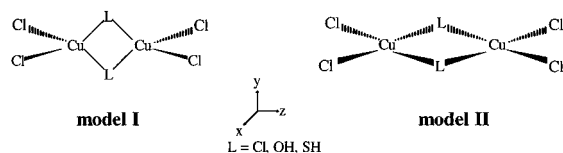
$$V_{ab} = \frac{1}{1 - S_{ab}^2} \left(H_{ab} - S_{ab} \frac{H_{aa} + H_{bb}}{2} \right) \quad (2)$$

where H_{aa} , H_{bb} , and H_{ab} are matrix elements for the representa-

(13) Landau, L. D. *Phys. Z. Sowjetunion* **1932**, *1*, 88; **1932**, *2*, 46. Zener, C. *Proc. R. Soc. London Ser. A* **1932**, *137*, 696; **1933**, *140*, 660.

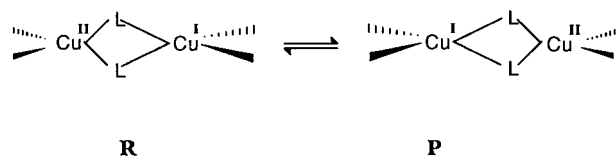
Table 1. Distances and Bond Angles (in Å and deg)^a

bridge	$d(\text{Cu}^{\text{I}}-\text{L})$	$d(\text{Cu}^{\text{II}}-\text{L})$	$d(\text{L}-\text{L})$	$\angle\text{L}-\text{Cu}^{\text{I}}-\text{L}$	$\angle\text{L}-\text{Cu}^{\text{II}}-\text{L}$	$\angle\text{Cu}-\text{L}-\text{Cu}$
OH	2.08	1.99	2.63	78	83	88
SH	2.38	2.3	3.49	95	99	83
Cl	2.34	2.25	3.39	93	98	85

^a Parameters for Cl bridge ligands taken from ref 1.**Figure 2.** Models used to represent the $[\text{Cl}_2\text{Cu}^{\text{I}}\text{L}_2\text{Cu}^{\text{II}}\text{Cl}_2]^{3-}$ mixed-valence system.

tion of the electronic Hamiltonian H on the basis of the nonorthogonal diabatic states Ψ_a and Ψ_b : $H_{aa} = \langle \Psi_a | H | \Psi_a \rangle$, $H_{bb} = \langle \Psi_b | H | \Psi_b \rangle$, $H_{ab} = \langle \Psi_a | H | \Psi_b \rangle$, and $S_{ab} = \langle \Psi_a | \Psi_b \rangle$. The diabatic states correspond to the charge-localized valence bond structures which characterize reactants and products, while the adiabatic states are the eigenfunctions of the electronic Hamiltonian. The computation of these quantities has been carried out using the corresponding orbital transformation¹⁴ as implemented in the HONDO8.4 program. For more details, see appendix of ref 15. As diabatic wave functions, the broken-symmetry unrestricted Hartree-Fock (UHF) solutions¹⁵⁻¹⁸ have been used.

The ab initio UHF calculations were undertaken with the use of the effective core potentials (ECP) proposed by Stevens et al.¹⁹ For Cu atoms the electrons explicitly described were those of 3s, 3p, 3d, and 4s shells, while for Cl, S, and O, only the valence electrons were taken into account. The basis sets used for these atoms were of double- ζ type for sp shells, and triple- ζ for Cu d orbitals. The contractions were (8s8p6d)/[4s4p3d] for Cu, and (4s4p)/[2s2p] for Cl, O, and S atoms. For hydrogen atoms, the standard (4s)/[2s] contraction of Dunning was chosen. With the aim to check whether the inclusion of either polarization functions or diffuse functions on the bridge atoms could affect the values of V_{ab} , some preliminary calculations with

(14) King, H. F.; Stanton, R. E.; Kim, H.; Wyatt, R. E.; Parr, R. G. *J. Chem. Phys.* **1967**, *47*, 1936.(15) Farazdel, A.; Dupuis, M.; Clementi, E.; Aviram, A. *J. Am. Chem. Soc.* **1990**, *112*, 4206.(16) (a) Cave, R. J.; Baxter, D. V.; Goddard, W. A., III; Baldeschwieler, D. *J. Chem. Phys.* **1987**, *87*, 926. (b) Broo, A.; Larsson, S. *Chem. Phys.* **1990**, *148*, 103. (c) Ohta, K.; Closs, G. L.; Morokuma, K.; Green, N. J. *J. Am. Chem. Soc.* **1986**, *108*, 1319. (d) Liang, C.; Newton, M. D. *J. Phys. Chem.* **1992**, *96*, 2855; **1993**, *97*, 3199. (e) Newton, M. D. *J. Phys. Chem.* **1988**, *92*, 3956. (f) Ohta, K.; Morokuma, K. *J. Phys. Chem.* **1987**, *91*, 401. (g) Durand, G.; Kabbag, O. K.; Lepetit, M. B.; Malrieu, J. P.; Marti, J. J. *Phys. Chem.* **1992**, *96*, 2162. (h) Naleway, C. A.; Curtiss, L. A.; Miller, J. R. *J. Phys. Chem.* **1991**, *95*, 8434.(17) Newton, M. D. *J. Phys. Chem.* **1986**, *90*, 3734.(18) Koga, N.; Sameshima, K.; Morokuma, K. *J. Phys. Chem.* **1993**, *97*, 13117.(19) Stevens, W. J.; Basch, H.; Krauss, M. *J. Chem. Phys.* **1984**, *81*, 6026. Stevens, W. J.; Krauss, M.; Basch, H.; Jasien, P. G. *Can. J. Chem.* **1992**, *70*, 612.**Figure 3.** Schematic representation of the electron-transfer process between Cu centers. The changes in the Cu-Cl bond lengths are overestimated to emphasize the nuclear relaxation taking place along the reaction.

larger basis sets were carried out on models I-Cl and II-Cl ($\alpha_d = 0.7$, $\alpha_{sp} = 0.0433$). Since the differences in V_{ab} were less than 5%, it was decided not to enlarge the basis set to speed up the calculations.

4. Results and Discussion

The ET reaction in the $\text{Cu}^{\text{I}}-\text{Cu}^{\text{II}}$ system is accompanied by a change in the geometry of the metal centers in order to accommodate to their new formal charge as shown in Figure 3. As stated above, V_{ab} is computed at a nuclear configuration corresponding to the crossing seam between the two diabatic surfaces; however, the determination of the geometry of such a point (the absolute minimum in the crossing region) is quite an involved task. Although computational procedures have been proposed to optimize the geometry of that point, in the present work this geometry was estimated assuming that the crossing seam corresponds to a symmetric nuclear configuration representing halfway between reactants and products. Effectively, within a $\text{Cu}_2\text{Cl}_4\text{L}_2$ unit, reactants and products can be considered as mirror images connected through a symmetric configuration corresponding to the transition state. This assumption can be substantiated, on the other hand, on the grounds of the Condon principle according to which the electronic coupling between two surfaces depends slightly on small coordinate variations.²⁰

This scheme allows for a straightforward definition of a reaction coordinate ξ which linearly mixes the geometries of reactants (Q_a) and products (Q_b) in such a way that

$$Q = \frac{\xi + 1}{2} Q_b - \frac{\xi - 1}{2} Q_a \quad (3)$$

where Q is the nuclear configuration at any point of the reaction path (for $\xi = -1$, $Q = Q_a$, lone electron localized on the left; for $\xi = 1$, $Q = Q_b$, lone electron localized on the right; the crossing seam occurs for $\xi = 0$).

Geometry Effects. Let us assume that the initial electronic arrangement corresponds to a $[\text{Cu}_2\text{Cl}_6]^{3-}$ unit in which the lone electron is localized on the left (Figure 3). The ground state for this complex corresponds to an open-shell configuration with the unpaired electron occupying a d_{yz} Cu^{II} orbital (${}^2\text{B}_2$ state). The ET reaction involves the jumping of an electron from the doubly occupied molecular orbital, MO, essentially built from the d_{yz} Cu^{I} atomic orbital toward the single occupied MO which essentially corresponds to the d_{yz} atomic orbital of Cu^{II} center. The jumping can occur, on the other hand, either

(20) Franck, J. *Trans. Faraday Soc.* **1925**, *21*, 536. Condon, E. U. *Phys. Rev.* **1925**, *32*, 858.

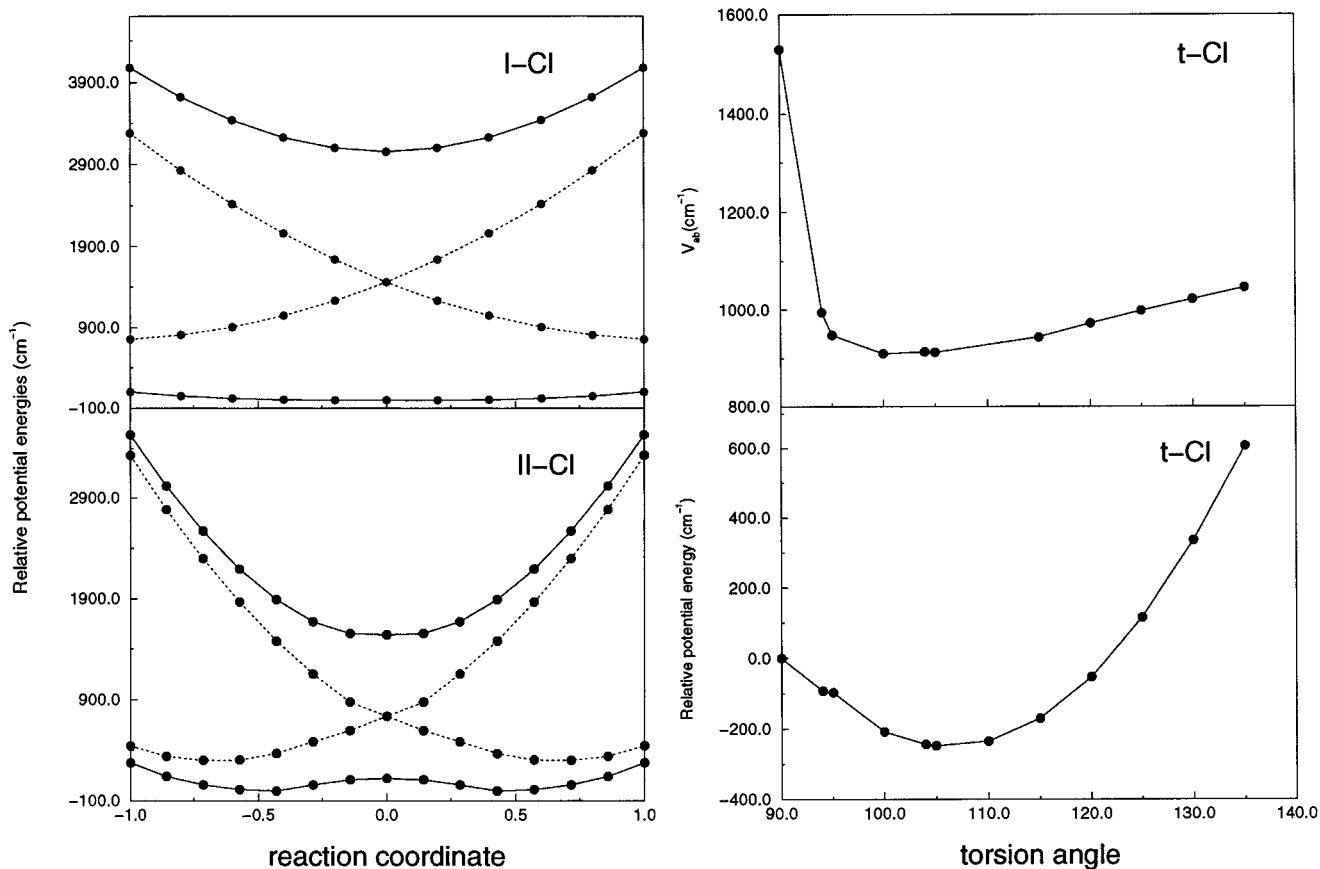
$\text{Cu}_2\text{Cl}_6^{-3}$ systems I-Cl, II-Cl, t-Cl

Figure 4. Left) Potential energy profiles for I-Cl and II-Cl models versus the reaction coordinate ξ . The solid lines correspond to the adiabatic states and the dashed lines to the diabatic ones. (Right) Variation at the crossing seam of the coupling and diabatic energies with respect to the torsion angle θ for model t-Cl.

through the crossing region or as a vertical transition between these ${}^2\text{B}_2$ states (the optical transfer). Concerning planar models, the single occupied MO is essentially the d_{xz} Cu^{II} orbital and the ET process involves a jumping from the doubly occupied d_{xz} Cu^{I} orbital, while the optical transfer occurs through a transition between ground and first excited ${}^2\text{B}_1$ states.

The potential energy surface cross sections for such ET processes, as a function of the reaction coordinate ξ , are reported for chloride derivatives in Figure 4. As can be seen, both models feature well-defined diabatic wells; however, there is a noticeable difference between these curves as while model I-Cl shows only one adiabatic minimum, model II exhibits two adiabatic minima. In other words, model I-Cl behaves as type III and model II-Cl as type II. The reason for this is due to the different balance between the reorganization energy and the electronic coupling for these models. The reorganization energy arises mainly from the change in the Cu-Cl bond distance on going from the seam toward the diabatic minima: there is a lengthening in the Cu^{II} -Cl bond distance and a shortening in the Cu^{I} -Cl one. Assuming that these nuclear relaxations are similar for both models, the different behavior would be governed by the magnitude of the electronic coupling. A relatively large electronic coupling would lead to type III behavior while for smaller couplings types II or I should be observed. Effectively, for cluster I-Cl, the calculation of the electronic coupling leads to a V_{ab} of 1528 cm^{-1} while for model II-Cl, V_{ab} is found to be 764 cm^{-1} (these values are those computed at the seam, but they change only moderately along the reaction path in agreement with the Condon principle.)

Let us now analyze the dependence on the dihedral angle θ between the $\text{Cu}^{\text{II}}\text{Cl}_2$ planes. First of all, it should be noted that model I-Cl is the closest one to that of the Willett system in which the two-state theory for ET reactions could be strictly applied since upon twisting, d_{xz} and d_{yz} orbitals mix and, in fact, we have to deal with a four state system ($2{}^2\text{B}_1 + 2{}^2\text{B}_2$). Bearing in mind that the two-state framework is no longer valid, we have looked for two well-localized partner states and analyzed the evolution of the diabatic energies E_{diab} at both the minima and the crossing seam geometries as well as the coupling element V_{ab} . Results for this twisted model, t-Cl, are also reported in Figure 4. Starting from model I-Cl, $\theta = 90^\circ$, E_{diab} decreases on increasing θ , reaching a minimum for $\theta = 105\text{--}108^\circ$. Notice that although these values are diabatic, the deviation of θ from the perpendicularity ($15\text{--}18^\circ$) is found to be in quite good agreement with the experiment ($\theta = 90 + 27^\circ$).

A similar evolution is found for V_{ab} , whose value rapidly decreases when the states are allowed to mix and then slowly increases for larger values of θ . At the geometry corresponding to the minimum of the diabatic energy, $\theta = 108^\circ$, V_{ab} is found to be 945 cm^{-1} . There are no experimental data on this particular system; however, this value agrees quite well with those reported, for instance by Westmoreland et al.^{2b} for half-met-L derivatives of hemocyanin. These authors found from spectroscopic analysis, and using the Hush formalism,²¹ values of V_{ab} ranging between 790 and 1200 cm^{-1} depending on the nature of the bridge.

(21) Hush, N. S. *Trans. Faraday Soc.* **1961**, 57, 155.

Table 2. Electron-Transfer Matrix Elements, V_{ab} , Adiabatic Activation Energies, E_{ad}^{\ddagger} , and Optical Transition Energies, E_{op} , for I-Cl, II-Cl, and t-Cl Models with Different Representations for the Environment (cm^{-1})

model	environment ^a	V_{ab}	E_{ad}^{\ddagger}	E_{op}	type ^b
I-Cl	without	1528		3060	III
	(0.1,0.2)	1538	294	4930	II*
	(0.2,0.4)	1553	1095	6100	II
	N	1514		3030	III
	N(0.1,0.2)	1524	210	4680	II*
	N(0.2,0.4)	1538	1014	5840	II
II-Cl	without	764	14	1890	II*
	(0.1,0.2)	764	290	3360	II*
	(0.2,0.4)	767	1137	5800	II
	N	725		1450	III
	N(0.2,0.4)	728	1084	5580	II
t-Cl ($\theta = 108^\circ$)	without	950	360	4186	II*
	(0.1,0.2)	938	853	5348	II
	(0.2,0.4)	966	1724	6666	II
	N	991	94	3952	II*
	N(0.2,0.4)	971	1486	6360	II

^a Values between parentheses correspond to q_1 and q_2 charges, N means that the calculation was done including the effect of the counterion (NET_4^+). ^b Type of mixed-valence system according to the Robin-Day classification. *Notice that although they are conventionally of type II, the adiabatic barrier is of the order or less than $k_B T$.

The lowering of V_{ab} together with the small increment in the reorganization energy for the t-Cl model, gives rise to the appearance of two adiabatic minima; however, as shown in Table 2, where the results obtained for Cl derivatives are

summarized, the adiabatic barrier, E_{ad}^{\ddagger} , is found to be too small (360 cm^{-1}) for a proper type II behavior. With respect to the optical transfer, the experimental electronic spectrum shows bands at 5800 , 10000 , and 15870 cm^{-1} , the latter being assigned to the intervalence charge transfer. From the adiabatic energies at the reactant (or product) configuration for the twisted model, the transition energy computed for this band is 4186 cm^{-1} , a value noticeably lower than the experiment, suggesting that the model needs to be improved.

Bridge Effects. Results obtained for the models in which the CuCl_2 subunits are bridged by the groups OH^- and SH^- are summarized in Figure 5 and Table 3. The energy profiles for compounds I-OH and I-SH show a clear dependence of the coupling on the nature of the bridge. Thus, for model I-OH, the coupling is small ($V_{ab} = 82 \text{ cm}^{-1}$), and the curves correspond to type I, while for I-SH $V_{ab} = 506 \text{ cm}^{-1}$, and a profile of type III is again observed. As already mentioned (see Table 2), on going from the perpendicular I-Cl to the planar II-Cl model, V_{ab} is found to be decreased by $\sim 50\%$. However, for II-OH there is a dramatic increment in the electronic coupling showing now type II behavior. On the other hand, model II-SH is found to be similar to the I-SH one. In summary, the change in the geometry around the metal centers involves a variation in the V_{ab} values whose size and direction depends largely on the bridge nature. Similar trends have been reported by Newton et al.¹⁷ in their analysis of the ET reactions occurring in $\text{Fe}^{2+/3+}$ and $\text{Ru}^{2+/3+}$ systems with NH_3 and H_2O ligands. These authors showed how the ligand nature as well as the character of the

$\text{Cu}_2\text{Cl}_4\text{L}_2^{-3}$ L=OH, SH systems

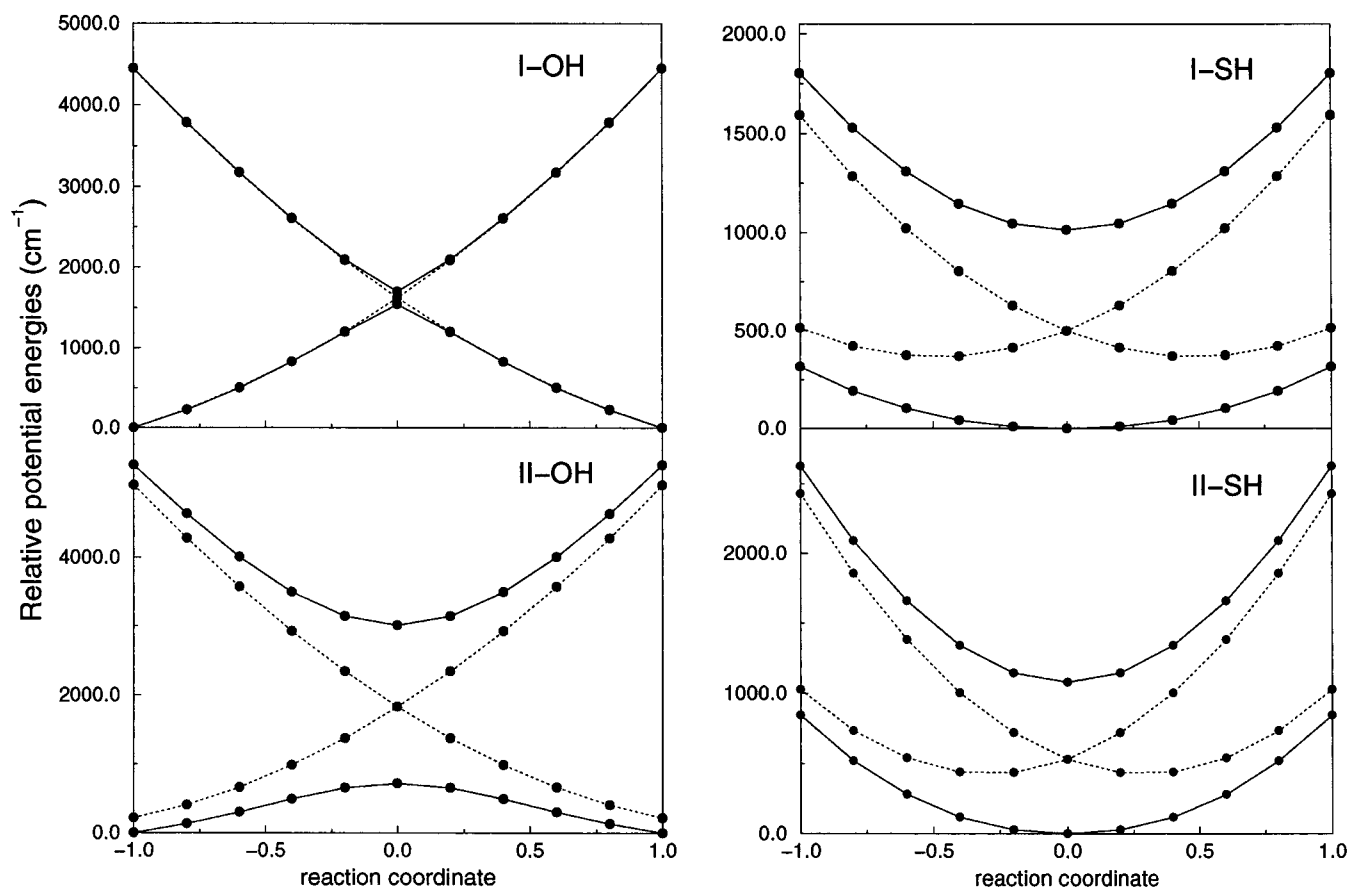


Figure 5. Potential energy profiles for OH and SH models versus the reaction coordinate ξ . Solid lines correspond to adiabatic states; dashed lines, diabatic.

Table 3. Electron-Transfer Matrix Elements, V_{ab} , Adiabatic Activation Energies, E_{ad}^{\ddagger} , and Optical Transition Energies, E_{op} for OH and SH (in cm^{-1})

model	environment ^a	V_{ab}	E_{ad}^{\ddagger}	E_{op}	type ^b
I-OH	without	82	1539	4450	II
	(0.1,0.2)	68	2168	5900	II
	(0.2,0.4)	56	3183	7500	II
II-OH	without	1143	734	5360	II
	(0.1,0.2)	1145	1294	6700	II
	(0.2,0.4)	1152	2238	8200	II
I-SH	without	506		1010	III
	(0.2,0.4)	534	594	3900	II
II-SH	without	539		1080	III
	(0.1,0.2)	547	14	1520	II*
	(0.2,0.4)	547	514	4150	II

^a Values between parentheses correspond to q_1 and q_2 charges. ^b Type of mixed-valence system according to the Robin-Day classification. *Notice that although they are conventionally of type II, the adiabatic barrier is of the order or less than $k_B T$.

active electron (either a t_{2g} or a e_g) determine the size of the electronic coupling.

A classical topic in the theoretical study of ET reactions is the analysis of the through-bond (TB) and through-space (TS) contributions to V_{ab} .⁹ The usual way to estimate the TS contribution is to compute V_{ab} in a similar system but without the bridge. Attempts to converge the SCF UHF procedure on the $\text{Cl}_2\text{Cu}-\text{CuCl}_2$ cluster for the present work failed, preventing us from using this type of analysis. An alternative approach to the TS contribution is possible if V_{ab} is computed for the 2B_1 states. Effectively, taking model I-Cl, the lowest 2B_1 state (only 3.9×10^{-4} hartree above the ground state), involves the lone electron occupying the d_{xz} copper orbitals, i.e., those perpendicular to the bonding rhomb, and therefore, it is expected that the ET will occur through a direct mechanism in which the electron jumps from a Cu d_{xz} orbital toward the other. The value of V_{ab} calculated for this state is only 86 cm^{-1} , suggesting that the TS mechanism is of minor importance in this system. This result agrees, on the other hand, with the large dependence of V_{ab} on the nature of the bridge, as already discussed.

To understand the effects of the bridge on the V_{ab} element, a careful examination of the main contributions is needed. With this purpose in mind an analysis, which roughly follows that performed by Koga et al.¹⁸ in their study of the ET reactions in methylene chains, was carried out. In principle, one can expect that the following approximate relationship is satisfied:

$$H_{ab} - S_{ab}H_{aa} \propto S_{ab} \quad (4)$$

and since S_{ab} is small, V_{ab} is proportional to the overlap between the diabatic Ψ_a and Ψ_b states S_{ab} . Actually, the following relation between V_{ab} and S_{ab} has been proposed by Newton:¹⁷

$$\frac{V_{ab}}{|S_{ab}|} (\text{cm}^{-1}) \approx 3 \times 10^4 \text{ cm}^{-1} \pm 10\% \quad (5)$$

Moreover, an ET reaction between a donor, D, and an acceptor, A, is a process involving not only the active orbitals among which the ET occurs but there is also an electronic rearrangement of the inactive orbitals (those whose occupation remains unchanged) because of the different polarization. In other words, if the diabatic wave functions Ψ_a and Ψ_b for initial and

Table 4. Relation between the Electron-Transfer Matrix Element, V_{ab} , and the Overlap of the Diabatic Wave Functions S_{ab}

model	V_{ab}^a	$ S_{ab} $	$ s_{ab}^{da} $	C^b	c^b
I-Cl	1528	4.51×10^{-2}	4.81×10^{-2}	3.4	3.2
I-OH	82	3.26×10^{-3}	3.48×10^{-3}	2.5	2.4
I-SH	506	1.45×10^{-2}	1.56×10^{-2}	3.5	3.2
II-Cl	764	2.29×10^{-2}	2.44×10^{-2}	3.3	3.1
II-OH	1143	3.48×10^{-2}	3.71×10^{-2}	3.3	3.1
II-SH	539	1.69×10^{-2}	1.81×10^{-2}	3.2	3.0

^a Same values that in Tables 2 and 3. ^b $C = 10^{-4} V_{ab}/|S_{ab}|$, $c = 10^{-4} V_{ab}/|s_{ab}^{da}|$.

final states are written in a compact form such as

$$\begin{aligned} \Psi_a &= |\text{core}_a d_a \bar{d}_a a_a| \\ \Psi_b &= |\text{core}_b d_b a_b \bar{a}_b| \end{aligned} \quad (6)$$

the core orbitals for each state undergo different relaxation effects and therefore they do contribute to S_{ab} . However, assuming that such a contribution is small, the two diabatic states differ only by one occupied orbital, the β -spin HOMO \bar{d}_a in state **a** and a_b in state **b**, and therefore, V_{ab} is proportional to the overlap between these two orbitals. Actually, in terms of the corresponding orbitals $\{\chi_i\}$, the overlap between Ψ_a and Ψ_b is simply written:

$$S_{ab} = \langle \Psi_a | \Psi_b \rangle = \prod_i^N s_{ab}^{ii} \quad (7)$$

where N is the number of occupied orbitals and s_{ab}^{ii} represents the overlap between the corresponding orbital pairs. In the present calculations these values were always found to be larger than 0.9 with the exception of the active pair, whose overlap $s_{ab}^{da} = \langle \chi_a^d | \chi_a^d \rangle$ is noticeably lower. According to this, S_{ab} can be approximated by s_{ab}^{da} as can be seen in Table 4 where both quantities are reported for the models considered here. In this table, the ratio between V_{ab} and either the whole overlap S_{ab} (C) or just the overlap among the active corresponding orbitals to s_{ab}^{da} (c) is also displayed showing how eq 5 holds in these systems.

The reduction from S_{ab} to s_{ab}^{da} involves a large benefit in the analysis of the ET process since this can now be performed in terms of the active β -spin HOMO corresponding orbitals χ_a^d and χ_b^a (i.e., from a one-electron point of view). On the other hand, these orbitals are, in our case, mirror images at the crossing seam. The contour maps of the χ_a^d orbitals for the six models are reported in Figure 6. Figure 6a,c,e corresponds to models I-Cl, I-OH, and I-SH, while Figure 6b,d,f are those of models II-Cl, II-OH, and II-SH, respectively. Starting with models of type I, it can be seen that these orbitals are mainly $\text{Cu}^{\text{II}} d_{yz}$ orbitals with orthogonality tails on Cu^{I} center; however, the tail is clearly larger for compound I-Cl, and therefore it seems obvious that the overlap with its corresponding orbital, mainly centered on Cu^{II} , has to be larger in agreement with its larger V_{ab} value. On the other hand, comparison of parts c and e of Figure 6 shows that understanding the differences between I-OH and I-SH is not only a matter of the size of the tails but that a more detailed analysis is needed. For this purpose it is useful to divide s_{ab}^{da} into one-center and two-

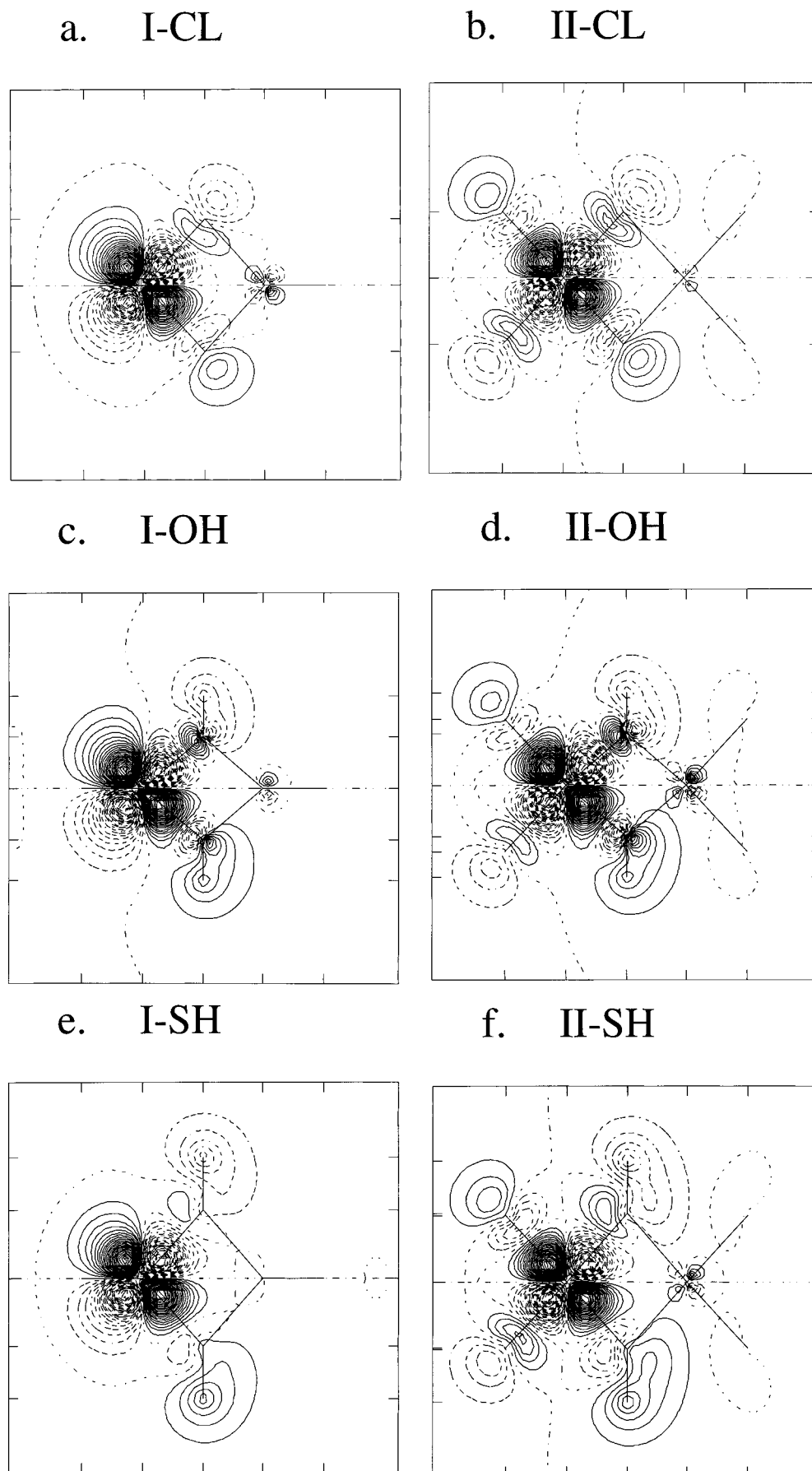
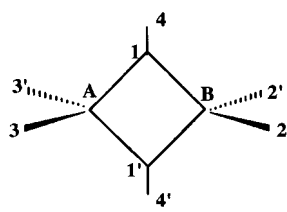


Figure 6. Active β -HOMO corresponding orbitals for the different models.

Table 5. One- and Two-Center Contributions to the Overlap between the Corresponding β -HOMOs of Diabatic Wave Functions


model	one-center ^a			two-center ^b					
	A	1(4)	2	A-B	A-1	A-2	A-3	A-4	1-4
I-Cl	0.0264	-0.0195	0.0008	-0.0136	0.0118	-4×10^{-5}	0.0004		
I-OH	0.0033	0.0091 (0.0049)	0.0013	0.0104	-0.0068	-2×10^{-5}	0.0009	0.0017	-0.0047
I-SH	0.0068	-0.0195 (0.0081)	0.0005	-0.0166	0.0131	-9×10^{-5}	-0.0002	-0.0018	0.0061
II-Cl	0.0106	-0.0173	0.0069	-0.0131	0.0129	-0.0001	-0.0029		
II-OH	0.0232	0.0072 (0.0047)	-0.0045	0.0124	-0.0077	-3×10^{-5}	0.0028	0.0016	-0.0051
II-SH	0.0201	0.0168 (0.0082)	-0.0071	0.0150	-0.0133	0.0003	0.0023	0.0009	-0.0059

^a For one-center overlaps: $1 = 1', 2 = 2' = 3 = 3', 4 = 4'$. ^b For two-center overlaps: $A-B = B-A, A-1 = A-1' = B-1 = B-1', A-2 = A-2' = B-2 = B-2', A-3 = A-3' = B-3 = B-3', A-4 = A-4' = B-4 = B-4', 1-4 = 1-4'$.

center contributions:

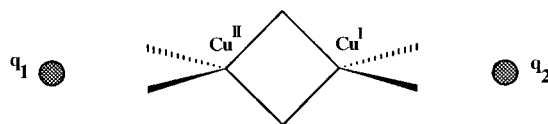
$$s_{ab}^{da} = \sum_I^{Nat} s_{ab}^I + \sum_{I < J}^{Nat} s_{ab}^{IJ} \quad (8)$$

where Nat is the number of atoms, and s_{ab}^I, s_{ab}^{IJ} the one- and two-center contributions, are computed using eq 13 of ref 18. The results are summarized in Table 5. As can be seen from this table, there are positive and negative contributions which correspond to in-phase and out-phase arrangements of the active orbitals. For I-SH, the one-center contribution arising from the metal atoms is almost twice that of I-OH but is largely compensated by the negative contribution arising from the bridge atoms (-0.0195 against 0.0091). The two-center metal-metal contribution for I-SH is also negative (-0.0166), thus diminishing the total s_{ab}^{da} , however, such contributions are clearly compensated by those due to the Cu-S pairs (A-1) which are positive (0.0131) while those of Cu-O are negative. A similar analysis can be performed on the planar models. The one-center Cu contribution for II-OH is an order larger than for I-OH in agreement with the larger value of V_{ab} computed for model II-OH. For compound II-Cl, this contribution decreases appreciably and since the remaining contributions are quite similar, V_{ab} lowers accordingly.

Environment Effects. The theoretical calculations on I-Cl and t-Cl models, those closer to the experimental system studied by Willet et al., give rise to an estimate of V_{ab} in good agreement with the proposed values for related systems but leads to a too small adiabatic barrier for the t-Cl model. This model also fails in the prediction of the optical transition. These failures suggest that a model based on isolated $Cu_2Cl_6^{3-}$ units is not good enough and that the influence of the rest of the chain as well as that of the counterions should be taken into account.

At first sight, the main limitation of the models is the lack of polarization along the chain direction. Such polarization could in principle be represented by introducing an electric field in the chain direction which, according to Farazdel et al.,¹⁵ would lead to a stabilization of the diabatic minima. The simplest way to represent this field is just to place point charges at the ideal copper positions both on the right and on the left of the models. However, the use of plain point charges to embed the

clusters is quite limited because it gives rise to an excessive polarization, since the electronic cloud can spread over them. For this reason, instead of using naked charges we have represented the two nearest copper ions by means of total ion potentials, TIPs, which hereafter will be denoted simply as q_1 and q_2 . These TIPs were described through a Cu large core Hay-Wadt effective core potential without basis functions:²²



The first problem to solve then is the choice of q_1 and q_2 since although in principle the formal charges $+1$ and $+2$ could be assumed, preliminary calculations showed that these values are too large since they give rise to an excessive stabilization of the minima leading to unrealistic adiabatic energies (-40 kcal/mol). These results suggested to us the use of partial charges obtained from a Mulliken population analysis. The Mulliken charge for copper ions computed at the seam is 0.27 for compound I-Cl (notice that at that point, both copper centers are equivalent) thus, a reasonable guess for q_1 and q_2 is 0.2 and 0.4 , which would lead to a charge of $q_1 = q_2 = 0.3$ at the crossing seam. This choice is, however, rather arbitrary and likely overestimated, so we have also tested a second set of charges namely 0.1 and 0.2 .

The results obtained with this embedded description for systems t-Cl, I-Cl, and II-Cl models are also included in Table 2. In the calculation of these energies, the charge of q_1 and q_2 is smoothly varied along the reaction coordinate, for instance from $(0.2, 0.4)$ to $(0.4, 0.2)$, according to a concerted and adiabatic electron transfer from Cu^I to Cu^{II} . As can be seen, the values of V_{ab} are slightly modified, showing that the electronic coupling is almost independent of the environment description in agreement with the theoretical results of Farazdel et al. as well as with experimental observations.²³

On the other hand, the interaction with the field induces a general stabilization of the system which increases with the field. At the crossing seam, this stabilization is mainly due to a

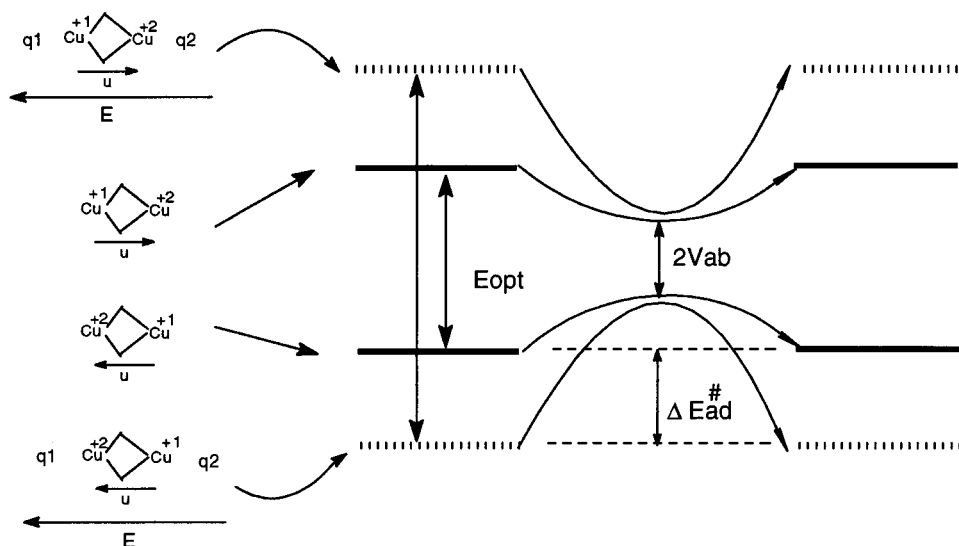


Figure 7. Summary of the environment effects on the energetic parameters at the minima and crossing seam regions. The lines correspond to the ground and first excited adiabatic states for reactants and products with (dashed) and without (full) the external electric field. The presence of the charges (q_1, q_2) stabilizes preferentially the ground state (and destabilizes the first excited state) in the minima region increasing E_{ad}^\ddagger and E_{op} .

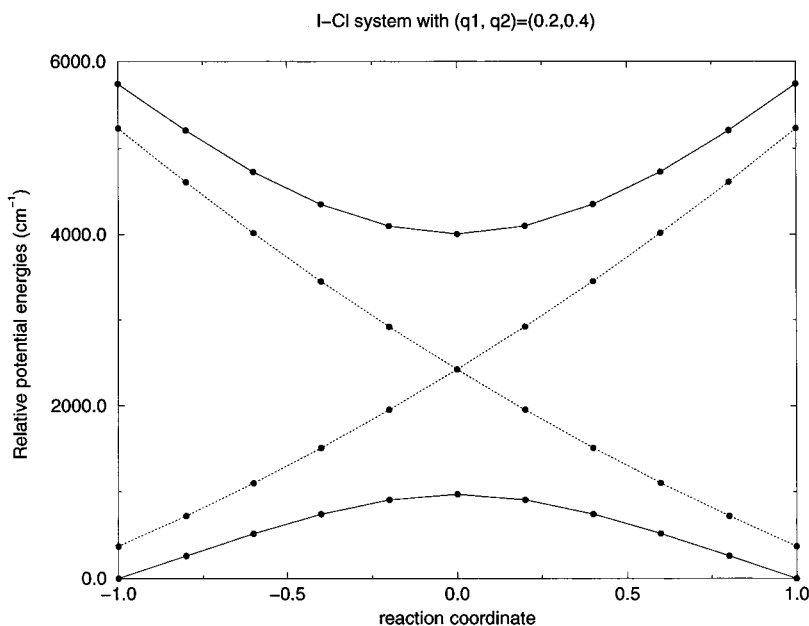


Figure 8. Potential energy profiles for I-Cl model versus the reaction coordinate ξ in the presence of the charges (q_1, q_2). Solid lines correspond to adiabatic states; dashed lines, diabatic.

polarization induced by the charges. However, out of the crossing seam, there is an additional stabilization due to the interaction of the electric field and the dipole moment of the cluster as sketched in Figure 7. This interaction produces an increment of the reorganization energy leading to a relative stabilization of the diabatic minima, and for an almost constant electronic coupling, to a relative stabilization of the adiabatic minima, E_{ad}^\ddagger , as shown for models t-Cl and II-Cl. Such a stabilization increases the adiabatic barrier, and this effect is larger when the charges increase. For model I-Cl, the incorporation of environment effects is more dramatic since now,

the reorganization energy becomes high enough to compensate the electronic coupling leading to a correct description as type II in the Robin–Day classification, as shown in Figure 8 where the energy profiles for the set (0.2, 0.4) are drawn. For the same reason, the energy for the optical transitions raises, leading to improved values, although they still are lower than the experimental ones. This discrepancy is likely due to the lack of electron correlation in the UHF wave functions. The effect of the electric field on the electron coupling and minima stabilization for models I-OH, II-OH, I-SH, and II-SH were also analyzed and the results are reported in Table 3.

A further interesting point in this analysis is to examine the dependence of the TB and TS contributions on the presence of the polarization field. As stated above, the TS contribution can be estimated by computing V_{ab} for 2B_1 states. It is found that V_{ab} diminishes by 10 cm^{-1} for set (0.1, 0.2) and by 29 cm^{-1} for set (0.2, 0.4). Although these values are numerically small,

(23) (a) Franzen, S.; Boxer, S. G. Manipulation of ET Reaction Rates with Applied Electric Fields. In *Electron Transfer in Inorganic, Organic and Biological Systems*; Bolton, J. R., Mataga, N., McLendon, G., Eds.; Advances in Chemistry Series 228; American Chemical Society: Washington, DC, 1991. (b) Crutchley, R. J. *Adv. Inorg. Chem.* **1994**, *41*, 273. (c) Pérez-Tejeda, P.; Benko, J.; López, M.; Galán, M.; López, P.; Domínguez, M.; Moyá, M. L.; Sánchez, F. *J. Chem. Soc., Faraday Trans.* **1996**, *92*, 1155. (d) Gramp, G.; Rauhut, G. *J. Phys. Chem.* **1995**, *99*, 1815.

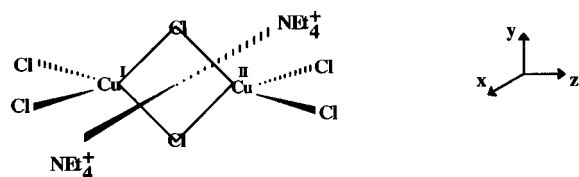


Figure 9. Schematic representation of the models including the effect of the $[\text{NEt}_4]^+$ counterions.

they represent the 11.6% and 33.7% of the TS contribution to V_{ab} , indicating a stronger dependence than for the TB one. These results can be rationalized on the grounds of the overlap differences induced by the electric field. Effectively, the presence of q_1 and q_2 polarizes the electronic density on the bonding rhomb lowering the wave function amplitude in this region for both ${}^2\text{B}_1$ and ${}^2\text{B}_2$ states, however, this effect is compensated in the ${}^2\text{B}_2$ states by the increment in the contribution arising from the ending Cu–Cl₂ groups.

The influence of the $[\text{NEt}_4]^+$ counterions will now be considered. The unit cell of $[\text{NEt}_4][\text{Cu}_2\text{Cl}_4]$ is constituted by two $(\text{Cu}_2\text{Cl}_4)_2$ chains and four $[\text{NEt}_4]^+$ cations with the ethyl arms fully extended, see Figure 1. As shown, the cations are grouped by pairs, and somewhat off-centered from the perpendicular line across the center of the CuCl_2Cu rhomb in such a way that the N–N line lies closer to Cu(I) centers. As for the Cu ions, the $[\text{NEt}_4]^+$ cations have been represented through an effective core potential without basis set and a charge of +0.5 which correspond to a formal charge of +1 shared by two chains. The profile energies for these models are computed assuming that at the crossing seam both copper atoms are equivalent and, therefore, at this point the two $[\text{NEt}_4]^+$ cations have to lie just on the perpendicular line to the rhomb center as depicted in the same Figure 9 for system I–Cl. This assumption would avoid any residual polarization along the z axis at the crossing seam, but just to include the effect of the field along the x direction.

The results for these calculations with and without q_1 and q_2 charges are also reported in Table 2, entries labeled by N. As found in the preceding section, the effect on the V_{ab} values for both I–Cl and II–Cl models is almost negligible, showing again the low dependence of the electronic coupling on the external field. However, some significant differences are observed on the potential surface shapes. Thus, in the absence of q_1 and q_2 charges, both I–Cl and II–Cl systems behave as type III, and the correct type II behavior is only obtained when the lateral charges q_1 and q_2 charges are introduced, except now, the adiabatic barriers are smaller. In other words, while the electronic coupling remains almost unchanged, the stabilization of the diabatic minima induced by the $[\text{NEt}_4]^+$ cations acts against that of q_1 and q_2 charges. These results can be understood by taking into account the electric field component along the z direction introduced by the $[\text{NEt}_4]^+$ cations. Thus, for reactants, $\xi = -1$, there is a net z component of the field, F_z , which now points in the *opposite direction* to the cluster dipole moment. Therefore, the diabatic minima are relatively less stabilized with respect to the crossing seam, $\xi = 0$, where $F_z = 0$. For a similar electronic coupling, the behavior of model II–Cl is changed from type II to type III. For mixed models ($[\text{NEt}_4]^+ + (q_1, q_2)$ charges), the z component of the electric field is dominated by (q_1, q_2) and type II for both models is again observed although with smaller adiabatic barriers E_{ad}^\ddagger .

Finally, some remarks concerning the methodology used here will be addressed. All the calculations have been carried out by exploiting the properties of the UHF broken-symmetry wave

functions. Although this procedure, commonly called as “diabatic”, is quite tedious, it allows the electronic coupling to be estimated at a reasonable computational cost. Also, as an additional benefit, it allows for an interpretation from a one-electron point of view. However, these diabatic states are not correlated, and one can wonder if electron correlation effects are significant enough to change our conclusions. To check this, we have performed single-point calculations on model I–Cl and t–Cl but using a correlated adiabatic approach. For this, we have computed the adiabatic energies at the crossing seam from density functional theory, DFT. For the exchange, the hybrid Becke’s three parameter functional was chosen,²⁴ while for correlation, we used the Lee, Yang, and Parr functional²⁵ (B3LYP). The values obtained were 1751 cm^{-1} and 975 cm^{-1} , which agree quite well with those reported in Table 2: $V_{\text{ab}} = 1528$ and 950 cm^{-1} . Therefore, it appears that, as far as the electronic coupling is concerned, the diabatic way seems a good choice, at least for the system here considered. Of course this is not the case for the electronic transitions where, as it is well-known, the effects of electron correlation are expected to be larger.

5. Concluding Remarks

In this paper we have carried out a theoretical analysis of some factors governing the electronic coupling in bridged $\text{Cu}^{\text{I}}-\text{Cu}^{\text{II}}$ mixed-valence compounds based on *ab initio* Hartree–Fock calculations. Starting with a basic model of formula $\text{Cl}_2\text{Cu}^{\text{I}}\text{L}_2\text{Cu}^{\text{II}}\text{Cl}_2$, the influence of the bridge, ($\text{L} = \text{Cl}^-, \text{OH}^-, \text{SH}^-$) and the local geometry around the Cu centers have been examined. The electronic coupling matrix element, V_{ab} , is found to be extremely sensitive to these structural parameters. Although interpretation of these results is quite involved, we have found how it can qualitatively be rationalized by examining the overlap between the active corresponding orbitals and, quantitatively, in terms of one- and two-center contributions according to the partition proposed by Koga et al. Also, the through-bond contribution is estimated to dominate the coupling in agreement with the observed dependence of V_{ab} on the bridge.

The computation of the energy profiles along idealized reaction coordinates for the electron transfer between Cu^{I} and Cu^{II} centers shows that it is necessary to include the effect of the surrounding copper cations to reproduce correctly the type II behavior within the Robin–Day classification reported by Willett for the $[\text{NEt}_4][\text{Cu}_2\text{Cl}_4]$ chains. We have shown how the inclusion of these polarization effects leads to stabilization of the adiabatic minima and to a better estimate of the intervalence charge-transfer electronic transition associated to the optical electron transfer. However, it still appears to be noticeably lower than the experimental value, likely due to the lack of electron correlation. The effect of $[\text{NEt}_4]^+$ counterions has also been examined and found to play only a minor role on the energy profiles although in the contrary sense to that of the surrounding copper ions. However, for a given model, both the presence of the counterions and the surrounding copper centers do not seem to modify significantly the electronic coupling but just the adiabatic barriers. This low dependence of the electronic coupling on the environment agrees with specific experiment in which a small influence of external electric fields on the electronic factor on ET reaction rates has been observed.^{23a} Also, these results agree with experimental kinetic findings according to which for a given donor–acceptor

(24) Becke, A. D. *J. Chem. Phys.* **1993**, *98*, 5684.

(25) Lee, C.; Yang, W.; Parr, R. G. *Phys. Rev. A* **1988**, *38*, 3098.

pair, the electronic coupling V_{ab} is found to be almost constant, and the different reaction rates observed are explained in terms of differential reorganization energies arising from the interaction with the solvent.^{23b-d}

Finally, the magnitude of the electronic coupling computed from UHF broken-symmetry wave functions has been compared with those obtained from higher level correlated calculations. It is found that the UHF values are at most 15% lower than those computed from DFT calculations. However, this aspect

deserves a more careful analysis, and work in this direction is currently being carried out in our laboratory.

Acknowledgment. This work was supported by the DGI-CYT (Spain, project no. PB95-1247), and by the European Commission (contract no. ERBCT1-CT94-0064). C.J.C. thanks the Ministerio de Educación y Ciencia for the award of a FPI grant.

JA972454A